Soft Matter

Accepted Manuscript

This article can be cited before page numbers have been issued, to do this please use: M. Khodeir, B. Ernould, J. Brassinne, S. Ghiassinejad, H. Jia, S. Antoun, C. Friebe, U. S. Schubert, Z. Kochovski, Y. Lu, E. van Ruymbeke and J. Gohy, *Soft Matter*, 2019, DOI: 10.1039/C9SM00905A.

ROYAL SOCIETY OF CHEMISTRY

rsc.li/soft-matter-journal

View Article Online
DOI: 10.1039/C9SM00905A

ARTICLE

Synthesis and characterisation of redox hydrogels based on stable nitroxide radicals

Received 00th January 20xx,
Accepted 00th January 20xx

DOI: 10.1039/x0xx00000x

Miriam Khodeir,[a] Bruno Ernould,[a] Jérémy Brassinne,[a] Sina Ghiassinejad,[a] He Jia,[a] Sayed Antoun,[b] Christian Friebe,[c] Ulrich S. Schubert,[c] Zdravko Kochovski,[d] Yan Lu,[d,e] Evelyne Van Ruymbeke [a] and Jean-François Gohy *[a]

The principle of encapsulation/release of a guest molecule from stimuli responsive hydrogels (SRHs) is mainly realised with pH, temperature or light stimuli. However, only a limited number of redox responsive hydrogels was investigated so far. We report here the development of a SRH that can release its guest molecule upon a redox stimulus. To obtain this redox hydrogel, we have introduced into the hydrogel the 2,2,6,6-tetramethyl-1-piperidinyloxy (TEMPO) stable nitroxide radical that can be reversibly oxidized into an oxoammonium cation ($TEMPO^+$). Water solubility is provided by the presence of the (oligoethyleneglycol)methacrylate (OEGMA) comonomer. The electrochemical and mechanical characterizations showed that those gels exhibit interesting physicochemical properties making them very promising candidates for practical use in a wide range of applications.

Introduction

Hydrogels have received considerable attention over the past 50 years due to their exceptional promise in a wide range of applications.[1] Hydrogels can be defined as polymer networks consisting of inter- and intra-molecularly connected polymer chains that possess the ability to absorb large amounts of water while maintaining their three-dimensional structure.[2] The stimuli-responsive hydrogels (SRHs), also called 'smart' hydrogels, represent a broad class of hydrogels being actively investigated, and some of them have been considered for practical use.[3,4,5] SRHs can be defined as hydrogels that are able to modify their equilibrium swelling in response to external stimuli such as pH,[6,7] temperature,[7,8] redox,[9,10] light,[11,12] and electrical field.[13]

A lot of work has been carried out on temperature-sensitive SRHs using poly(N-isopropyl acrylamide) (PNIPAM) as thermo-responsive unit. Indeed, PNIPAM exhibits a lower critical solubility temperature (LCST) around 32 °C in aqueous medium and is therefore very useful for preparing smart materials for biological applications.[14,15,16,17] However, in recent years, scientists reported very interesting alternatives to PNIPAM. New families of polymers exhibiting either LCST or upper critical solubility (UCST) behaviors in water have been described in the literature.[18,19,20,21] Among them, thermo-responsive polymers containing short oligo(ethylene glycol) side-chains have gained rapid success in fundamental polymer science but also in applied materials research.[21] Early reports by Aoshima and co-workers [22] and Ishizone and co-workers[23] demonstrated that some of those polymers exhibit a LCST behavior in aqueous medium. It was afterwards shown that these stimuli-responsive properties can be finely adjusted via macromolecular design, and in particular using co-polymerization approaches.[24,25,26]

As far as redox responsive SRHs are concerned much less work has been performed. Hydrogels based on disulphide cross-linkers can be cited, where the gels dissolve and release their guest molecules when the disulphide bonds are broken.[27] Other systems involve ferrocene functions that can change the hydrophilic-hydrophobic balance of the gel depending on the redox state of the ferrocene moieties.[27,28] Other examples of redox responsive polymers involve conducting polymers, such as polyaniline (PANI) or polypyrrole (PPy), where clusters of conductive polymer are entrapped into the hydrogels. When submitted to an electrical current the conducting polymer becomes hydrophilic and allows the encapsulated drug to diffuse out of the hydrogel.[29,30]

Our strategy in this contribution is to design a redox responsive hydrogel that can encapsulate negatively charged hydrophilic molecules upon oxidation and release them upon reduction. To obtain this redox responsive hydrogel, we decided to focus our attention on the 2,2,6,6-tetramethyl-1-piperidinyloxy (TEMPO) group as redox-active component. TEMPO is a stable nitroxide radical that can be easily oxidised into its oxoammonium counterpart or reduced into an aminoxyl functions.[31] Nitroxide radicals, and especially TEMPO derivatives, are largely used in chemistry for the

[a] Institute of Condensed Matter and Nanosciences (IMCN), Bio and Soft Matter (BSMA), Université catholique de Louvain (UCL), Place L. Pasteur 1 & Croix du Sud 1, B-1348 Louvain-la-Neuve, Belgium. Email : jean-francois.gohy@uclouvain.be
[b] Department of chemistry, Faculty of science section III- North campus-Tripoli, Lebanese university (UL), Lebanon
[c] Laboratory of Organic and Macromolecular Chemistry, Friedrich- Schiller-Universität Jena, Humboldtstrasse 10, 07743 Jena, Germany
[d] EM-ISFM Soft Matter and Functional Materials, Helmholtz-Zentrum Berlin für Materialien und Energie, Hahn-Meitner-Platz 1, 14109 Berlin, Germany
[e] Institute of Chemistry, University of Potsdam, 14476 Potsdam, Germany
†Electronic Supplementary Information (ESI) available: Library of gels, NMR spectra, FTIR spectra and Swelling factor for different X_{CL}. See DOI: 10.1039/x0xx00000x

DOI: 10.1039/C9SM00905A

synthesis of organic molecules or polymers,[32] and in the biomedical field as imaging enhancer in electron spin resonance (ESR) techniques or as radical scavenger of reactive oxygen species (and thus anticipated as valuable candidates for anti-oxidant therapies).[33] Moreover, the redox equilibrium associated to nitroxide radicals, and especially TEMPO, has been used in the recent years for the production of energy storage devices.[34,35] For the energy storage application, scientists developed a polymer bearing TEMPO moieties, poly(TEMPO methacrylate) abbreviated as PTMA.[34] In the present work, we have introduced this polymer into a hydrogel in order to produce redox responsive SHRs.

A precursor of the hydrogel will be firstly synthesized by conventional radical polymerisation. This polymeric network will be obtained from a mixture of 2,2,6,6-tetramethylpiperidin-4-yl methacrylate (TMPM), oligo(ethylene glycol) methyl ether methacrylate with an average molar mass of 300 g/mol ($OEGMA_{300}$) and di(ethylene glycol) dimethacrylate ($OEGMA_2$) as cross-linker. In the second step, the secondary amine of TMPM units will be oxidised into TEMPO-methacrylate **(**TEMPO) to obtain the desired redox responsive hydrogel. The final step will be the oxidation of the nitroxide radical units of TEMPO into oxoammonium ones ($TEMPO^+$). In this case the encapsulation of the molecules would be driven by electrostatic interactions between the anionic molecules and the positively charged $TEMPO^+$ units of the hydrogels. The reduction of the $TEMPO^+$ into TEMPO will finally allow the disappearance of those electrostatic interactions and thus the diffusion of the guest molecules out of the hydrogel (Fig. 1).

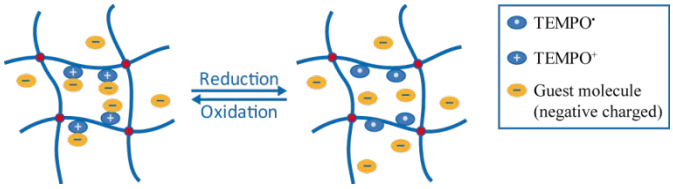

Fig. 1 Schematic representation of redox hydrogels for the encapsulation/release of negatively charged molecules.

Experimental

Materials and methods

All chemicals and monomers were purchased from Aldrich, Fluka, or Acros. Solvents were bought from Acros. Poly(ethylene glycol) methyl ether methacrylate (POEGMA, average molar mass of 300 g/mol, Aldrich) and di(ethylene glycol) dimethacrylate ($OEGMA_2$, Aldrich) were purified on a AlO_x-filtration column prior use in order to remove the inhibitor. The 2,2'-aziobutyronitrile (AIBN, 98% purity, Fluka) initiator was recrystallized twice from methanol prior use.

Instrumentation

^{1}H NMR spectroscopy. Proton nuclear magnetic resonance (^{1}H NMR) spectra were acquired on a 300 MHz Bruker Avance II in deuterated chloroform from the supernatant of the polymerization medium and in acetonitrile for the hydrogel obtained after polymerization. ^{1}H NMR spectra were also recorded in the presence of an internal standard on the soluble fraction of oxidized gels swollen with an excess of D_2O in order to determine the fraction of chains that were not entrapped in the network.

Size exclusion chromatography (SEC). Apparent average molar masses (M_n and M_w) and dispersity ($Đ$) were measured on an Agilent SEC system equipped with an Agilent 1100/1200 pump (25 °C, eluent: chloroform/triethylamine/isopropanol (94/4/2), flow rate: 1 mL.min-1), an Agilent differential refractometer and two PSS SDV columns (1000 Å and 10000 Å). The calibration was performed using poly(methyl methacrylate) standards.

Fourier-transform infrared spectroscopy (FTIR). FTIR spectra were recorded with a Shimadzu FTIR-8400S spectrometer. The dried oxidized and reduced hydrogels were ground with KBr and pressed into pellets under reduced pressure.

UV-visible (UV-Vis) spectroscopy. After equilibration of the oxidized hydrogel swelled in eosin B solution, the supernatant was transferred into quartz cuvettes and measured in a Varian Cary 50 UV-Vis spectrophotometer with emission scans recorded from 250 to 800 nm.

Rheological measurements. Rheology experiments were performed on a Kinexus Ultra (Malvern Instruments) rheometer equipped with a heat exchanger and modified with a solvent trap. Measurements were carried out using a plate-plate steel geometry (8 and 20 mm diameter) with a gap adjusted between 450 and 1800 µm so that the geometry was completely filled. Oscillatory measurements were carried out in the linear regime (either at strain control of 1% or at stress control of 5 Pa). Strain sweep measurements have also been performed at a strain amplitude ranging from 0.3% to 1000% and at a frequency of 5 rad/s. Measurements were carried out at 20 °C, in a water saturated atmosphere in order to minimize evaporation of the solvent. Normal forces were checked to be relaxed to <0.05 N prior any measurement.

Swelling tests. The dry gels were swollen in distilled water at 25 °C in an isothermal water bath to study the equilibrium swelling kinetics. Mass measurements were taken at time points of 0, 0.5, 1, 2, 4, 8, 24, and 48h. The swelling factor was defined as the weight ratio between the difference in hydrogel weight in both dry and swollen state over the weight of the dry gel.

Electron Spin Resonance (ESR). The EPR spin count was determined as the mean value achieved from the EPR spectra of three samples of the TEMPO-containing gel. For comparison, the EPR spin count of a TEMPO-free gel was determined likewise. X-band EPR spectra were acquired on an EMXmicro CW-EPR spectrometer from Bruker, Germany (EMX micro EMM-6/1/9-VT control unit, ER 070 magnet, EMX premium ER04 X-band microwave bridge equipped with EMX standard resonator, EMX080 power unit). The samples were investigated at room temperature and the data handling was done with the Bruker Xenon software package, version 1.1b86. The SpinCountQ software module was used for the determination of the spin count.

Electrochemical measurements. Charge/discharge tests were performed using an ARBIN Instrument Battery Tester (BT-2043). The cyclic voltammetry (CV) tests were carried out using a Parstat 3000. The CV measurements were performed at a scan rate of 0.1 mV/s. The electrodes were tested in half-cell configuration with lithium

metal foil as counter and reference electrodes and porous polyethylene membrane as separator. The electrolyte used was 1 M of lithium hexafluorophosphate (LiPF6) in ethylene carbonate (EC) and diethyl carbonate (DEC) (1:1, v:v). All coin-cells were assembled under argon atmosphere (<0.1 ppm H_2O, <0.1 ppm O_2) in an Inert Lab glovebox.

Electrode preparation. The cathodes were prepared by blending the active gel material, conductive carbon black (Super C45, MTI), carboxymethyl cellulose (CMC) and Styrene-Butadiene Rubber (SBR) binder. The blend has the following composition, 60 wt. % of PTMA, 25 wt. % of carbon black and 5:10 wt. % of CMC:SBR binder. The ingredients were mixed uniformly at room temperature for 4 hours to yield the slurry. The slurry was cast on an aluminum foil using the doctor blade method (the thickness of the wet film was controlled to be 30 µm) and dried at 60 °C. Circular discs of 1 cm diameter were cut and used as cathodes for evaluating the electrochemical properties. Disks were subsequently punched and pressed at 6 tons/cm^2. Prior the cell assembly, the electrode was dried at 55 °C in vacuum for 12 hours. The coating mass was typically 0.5 to 1.5 mg/cm^2.

Cryogenic-transmission electron microscopy (Cryo-TEM). Samples for cryo-electron microscopy (cryo-EM) were prepared by applying a 4 µl droplet of diluted sample suspension to lacey carbon copper grids (200 mesh, Science Services) and plunge frozen into liquid ethane using a Vitrobot Mark IV(FEI, Eindhoven, Netherlands)set at 4°C and 95 % humidity. Vitrified grids were mounted on a cryo transfer holder (Gatan 914, Gatan, Munich, Germany) and transferred into a JEOL JEM-2100 (JEOL GmbH, Eching, Germany) transmission electron microscope for imaging. The microscope was operated at an acceleration voltage of 200 kV and a defocus of the objective lens of about 1.5–2 µm was used to increase the contrast. Micrographs were recorded with a bottom-mounted 4*4k CMOS camera (TemCam-F416, TVIPS, Gauting, Germany) at a magnification of 50 000x, corresponding to a pixel size of 2.32 Å at the specimen level. Total electron dose for each micrograph was kept below 20 e$^-$/Å^2.

Synthesis

Typical procedure for the precursor poly(2,2,6,6-tetramethylpiperidin-4-yl methacrylate-random-oligoethyleneglycol methacrylate) (P(TMPM-*r*-OEGMA)) hydrogel synthesis. The synthesis of the polymeric network was carried out using conventional radical polymerization. Into a 50ml round-bottom flask, TMPM (different molar ratios of TMPM/(TMPM+OEGMA) (abbreviated as X_{TEMPO} in the following)) were investigated 0.1, 0.2, 0.3 and 0.4) was dissolved in 2-propanol (IPA, 70 wt%), then OEGMA, $OEGMA_2$ (abbreviated as X_{CL}= $OEGMA_2$/(TMPM+OEGMA)) was also varied (0.014, 0.02, 0.03, 0.04 and 0.05) and the initiator AIBN (0.5 eq.) were added and stirred until homogeneous blending. The solution was then degassed by three freeze pump-thaw cycles and filled with argon before it was stirred in an oil bath at 70 °C overnight. A transparent gel was formed.

Typical procedure for the poly(2,2,6,6-tetramethylpiperidinyloxy methacrylate-random-oligoethyleneglycol methacrylate) (P(TEMPO-*r*-OEGMA)) hydrogel synthesis. The secondary amine of TMPM units has been oxidized into a nitroxide radical to lead to TEMPO. For that, the remaining IPA of the polymerization gel solution was removed under reduced pressure. Then Na_2WO_4 (0.25 eq.), EDTA (0.15 eq.) and methanol were added and the gel was swollen for a couple of hours before adding the oxidizing agent H_2O_2 (5eq.). The mixture was then stirred at 60°C overnight. An orange colored gel was obtained and washed four times with distilled water and methanol (1:1, v:v) and dried in vacuum at 40 °C overnight. An orange sticky gel was finally obtained.

Typical procedure for the oxidized (P(TEMPO$^+$-*r*-OEGMA)) hydrogel synthesis. The dried P(TEMPO-*r*-OEGMA) hydrogel was swollen in distilled H_2O (31.25 eq.). Then fluoroboric acid (HBF_4, 1 eq.) was slowly added dropwise over 1h at room temperature. After that, sodium hypochlorite (NaClO, 0.5 eq.) was added over 1h at 0°C and stirred for an additional 1h at 0°C to lead to the oxidized hydrogel P(TEMPO$^+$-*r*-OEGMA).[36] Then the hydrogel was washed with ice-cold 5 wt% $NaHCO_3$, aqueous solution and ice-cold diethyl ether. The obtained yellow gel was finally dried overnight at 40°C in vacuum.

Results and discussion

Synthesis and material characterization

The investigated P(TEMPO$^+$-*r*-OEGMA) hydrogels were synthesized via a three-step methodology as depicted in Fig. 2. First, a P(TMPM-*r*-OEGMA) precursor hydrogel was prepared by conventional radical polymerization, followed by the oxidation of the secondary amine of PTMPM units with H_2O_2 in methanol[37] to obtain the P(TEMPO-*r*-OEGMA) hydrogel. Different molar ratios of TMPM/(TMPM+OEGMA) (abbreviated as X_{TEMPO} in the following) were investigated (0.1, 0.2, 0.3 and 0.4) and the cross-linker molar ratio $OEGMA_2$/(TMPM+OEGMA) (abbreviated as X_{CL} in the following) was also varied (0.014, 0.02, 0.03, 0.04 and 0.05) to investigate both the influence of increasing TEMPO content and the density of cross-linker on the characteristics of the hydrogels (see Table S1, ESI†). Finally, the nitroxide radical units of TEMPO were oxidized into oxoammonium units (TEMPO$^+$) with NaClO in the presence HBF_4 to obtain the oxidized P(TEMPO$^+$-*r*-OEGMA) hydrogel.[38]

^{1}H NMR spectra of the supernatant of the polymerization medium were systematically recorded in order to monitor the polymerization reaction leading to the P(TMPM-*r*-OEGMA) precursor hydrogel. As a typical example, the ^{1}H NMR spectrum of the supernatant of the polymerization medium for the P(TMPM-*r*-OEGMA) hydrogel prepared with X_{TEMPO} = 0.4 and X_{CL} = 0.03 is shown in Fig. S1 after overnight polymerization. This spectrum reveals no vinyl peaks (around 4.6 - 6.5 ppm) indicating a full consumption of the monomers according to the precision limit inherent to ^{1}H NMR spectroscopy. In addition, the ^{1}H NMR spectrum of the P(TMPM-*r*-OEGMA) precursor network swollen in deuterated acetonitrile in the NMR tube (Fig. S2, ESI†) revealed a network composition corresponding to the comonomers feed and hence demonstrating

the complete incorporation of the comonomers into the synthesized network. Same results were obtained for all the synthesized networks presented in this work.

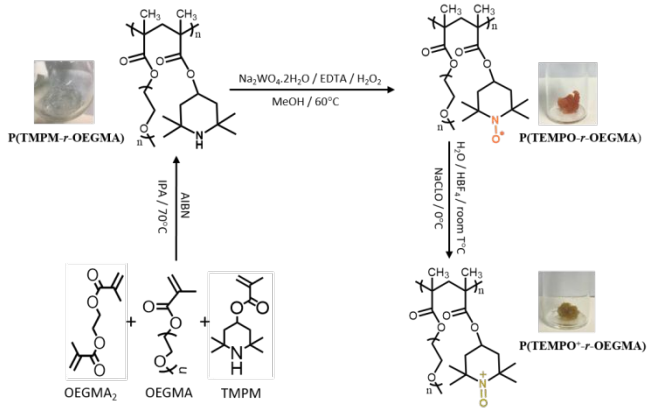

Fig. 2 Synthesis of P(TEMPO$^+$-*r*-OEGMA) hydrogels.

Cryogenic-transmission electron microscopy (Cryo-TEM) was used to obtain details about the microstructure of these hydrogels. As shown in Fig. S4 (ESI†) for a X_{TEMPO} = 0.2 and X_{CL} = 0.03 system, long nanowire-like structures were observed in the hydrogel. Spherical aggregates with diameters of 10 nm were also found doped around the long nanowires. These structures suggest the aggregation of some insoluble units into insoluble domains. Indeed, a similar microstructure was found by Zhai et al.[39] for hydrogels formed from β-cyclodextrin and an anionic surfactant containing a biphenyl group and in which the formation of hydrophobic nanodomains was also hypothesized. In our case, we believe that TEMPO units are at the origin of those hydrophobic domains. Indeed, TEMPO groups are basically hydrophobic and not water-soluble. The TEMPO groups randomly located in the P(TEMPO-*r*-OEGMA) network could then aggregate into hydrophobic domains making our system a combination of a chemically crosslinked hydrogel (through the $OEGMA_2$ units) and a physically crosslinked hydrogel (through the TEMPO hydrophobic domains).

Electrochemical Properties

The oxidation of the P(TMPM-*r*-OEGMA) precursor into the P(TEMPO-*r*-OEGMA) hydrogel was macroscopically observed by the apparition of the orange color characteristic of the nitroxide radicals (Fig. 2). The oxidation yield of TEMPO radical units to oxoammonium ones was further determined by ESR. This method indicates an oxidation yield of ca. 99% and confirms that a high rate of oxidation has been reached for all the investigated hydrogels. As a typical example, Fig. 3 (red line) shows for the P(TEMPO-*r*-OEGMA) hydrogel with X_{TEMPO} = 0.4 and X_{CL} = 0.03 a spin density of around 1.15×10^{-3}mol/g with the typical signal shape for polymeric organic radicals that confirms the presence of TEMPO radicals in this hydrogel.

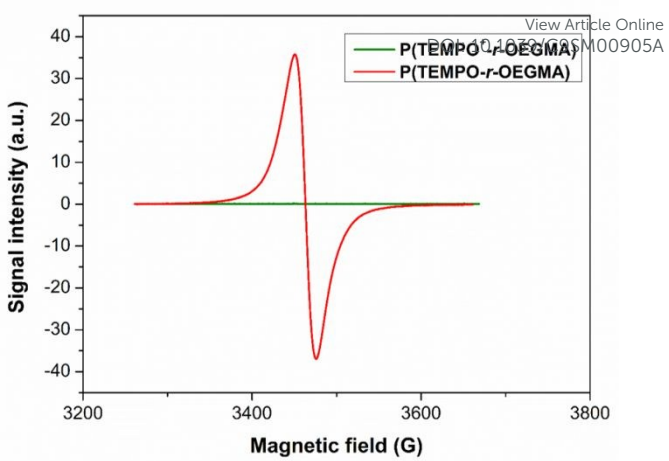

Fig. 3 Electron spin resonance spectra of the P(TEMPO-*r*-OEGMA) (red line) and P(TEMPO$^+$-*r*-OEGMA) (green line) hydrogels.

Finally, the P(TEMPO-*r*-OEGMA) hydrogels were converted into P(TEMPO$^+$-*r*-OEGMA) ones by the chemical oxidation of the nitroxide radicals into oxoammonium cations using NaClO. This reaction can be visually monitored by the change of color of the hydrogel from orange to yellow (Fig. 2). ESR was also used to monitor this reaction. As a typical example, a spin ratio of ca. 10^{-6} mol/g was measured for the P(TEMPO$^+$-*r*-OEGMA) hydrogel with X_{TEMPO} = 0.4 and X_{CL} = 0.03 and no characteristic signal belonging to radical species was clearly visualized (Fig. 3, green line). From the spin density measurement, we deduce that only ca. 0.1% of the TEMPO units are not oxidized into TEMPO$^+$, which practically means that the conversion of TEMPO units into TEMPO$^+$ ones is quantitative. Similar results have been obtained for all the investigated hydrogels.

Beside chemical oxidation of the P(TEMPO-*r*-OEGMA) hydrogels into P(TEMPO$^+$-*r*-OEGMA) ones, the redox reactions occurring in those materials can also be electrochemically triggered. To this aim, cyclic voltammetry measurements (CV) were performed to firstly confirm the presence of redox responsive TEMPO groups in our materials and secondly to study the reversibility of the redox reactions. Since performing the CV experiments directly with the hydrogels was not possible with our experimental set-up, we have used a methodology previously optimized for the investigation of TEMPO-containing polymer in Li-ion battery applications.[40] Practically, this means that the CV experiments have been performed in the solid state with an electrode prepared by blending P(TEMPO-*r*-OEGMA) or P(TEMPO$^+$-*r*-OEGMA) dried samples with conducting carbon black, in half-cell configuration against a metallic lithium counter electrode used as reference. Fig. 4 shows the reversible oxidation (blue line) of the nitroxide radicals into the oxoammonium cations for P(TEMPO-*r*-OEGMA) and the reversible reduction (red line) of the oxoammonium cations into nitroxide radicals for P(TEMPO$^+$-*r*-OEGMA) both around 3.6V vs Li/Li$^+$ with well-defined peaks for the samples prepared with X_{TEMPO} = 0.3 and X_{CL} = 0.03. This confirms the presence of TEMPO groups in our hydrogels and the reversibility of the redox processes associated to these groups. Similar results have been obtained for all the investigated samples evidencing their reversible redox responsive behavior.

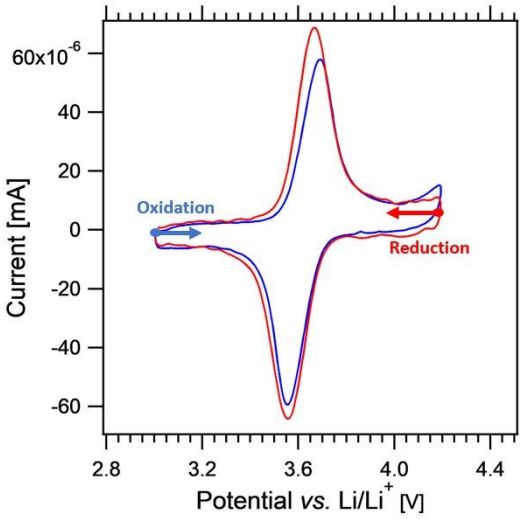

Fig. 4 Cyclic voltammetry of P(TEMPO-*r*-OEGMA) (in blue) and P(TEMPO⁺-*r*-OEGMA) (in red) electrodes in half-cell configuration with lithium as counter electrode at 0.5 mV/s (1 cycle is depicted for each electrode).

Mechanical properties

Swelling studies

Swelling tests were then performed on the P(TEMPO-*r*-OEGMA) hydrogels (Fig. 5, Fig. S5 and Table S1, ESI†). The swelling factor, defined as $[(Ws - Wd)/Wd]$ where w_s is the weight of hydrogel in the swollen state at the equilibrium and w_d is the weight of the hydrogel in the dry state, was measured as a function of X_{TEMPO} and X_{CL}. The equilibrium state was determined by regularly weighting the hydrogel during the swelling process until it reached a constant weight. This was typically achieved after 24h (Fig. 5a). However, the hydrogels were further equilibrated to reach a total time of 48h before measurement, to be sure to be at the equilibrium. The best results in terms of swelling factors and structure of the gels were obtained for X_{CL} = 0.03 (see Fig. S5, ESI†). Lower X_{CL} eventually leads to viscous fluids instead of gels (Table S1, ESI†) and lower swelling factors are observed for higher X_{CL} (Fig. S5, ESI†). Those results can be easily understood while taking into account that a too low concentration in crosslinking units impedes the formation of a continuous network of polymer chains in the hydrogel while a high concentration of those groups reduces the mesh size and is detrimental to high swelling ratio. In this respect, X_{CL} being equal to 0.03 seems to be the best compromise. Indeed, P(TEMPO-*r*-OEGMA) hydrogels with varying X_{TEMPO} ratio and X_{CL} fixed to 0.03 display swelling factors around 35 for X_{TEMPO} 0.1 and 0.2 (Fig. S5, ESI†), meaning that 0.025 g of dry sample adsorb around 1 g of water. And for X_{TEMPO} 0.3 and 0.4 the swelling factor decreases by nearly a factor of two, which can be explained by the increase in hydrophobicity provided by the TEMPO units. In addition, the fraction of chains which are not trapped in the network has been experimentally determined by preparing the P(TEMPO-*r*-OEGMA) gels with X_{TEMPO} of 0.1, 0.2, 0.3 and 0.4 with an excess of D_2O compared to the previously determined swelling ratios at equilibrium (Fig. 5). After equilibration for 48h, gels with a supernatant sol fraction were obtained. The amount of free chains released by the network has been further determined by measuring the amount of chains extracted in the sol fraction using ^{1}H NMR with an internal standard. This amount is approximately the same in the four analyzed samples and is 10.6 +/- 0.5 wt%. The same experiment was performed for the reference P(OEGMA) gel with X_{TEMPO}=0 and an amount of 20.5 wt% was determined.

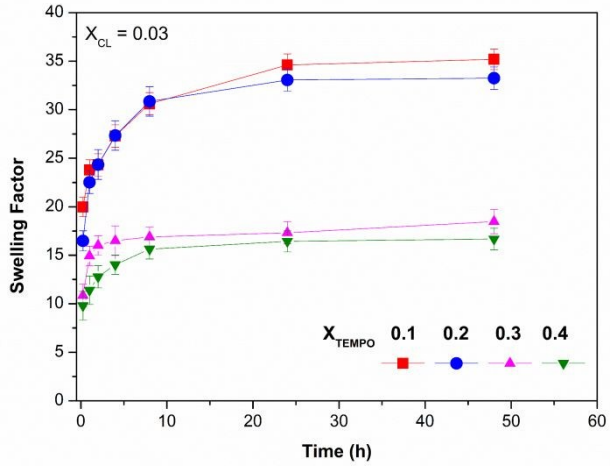

Fig. 5 Kinetic swelling study of P(TEMPO-r-OEGMA) hydrogels with varying XTEMPO , error bars represent average swelling ratio ± standard deviation where n = 3.

Rheological properties

The viscoelastic properties of the P(TEMPO-*r*-OEGMA) hydrogels were also investigated by rotational rheometry. In a first step, we tried to determine the gelation points by using the well-known Winter-Chambon methodology. However, due to the high dilution of the polymer chains in our hydrogels we could not measure the relaxation of the free chains nor the high frequency region of the storage and loss moduli, corresponding to the relaxation of the dangling ends. Thus, only the low frequency plateau modulus could be accessed which only tells about the number density of strands participating to the network.

According to the visual observations (Table S1, ESI†) only hydrogels with X_{CL} fixed to 0.03 were further investigated. Their viscoelastic response was measured as a function of the oscillation frequency for the different X_{TEMPO} values. As shown in Fig. 6, the storage modulus (G') is superior to the loss modulus (G") in the whole experimental frequency window, confirming the formation of a gel. Nevertheless, without TEMPO, the level of the storage modulus of the hydrogel is very low (~150 Pa), which suggests that the gel contains only few chemical crosslinks which effectively contribute to the polymer network. Based on the modulus, the average molar mass between two active crosslinks, M_{XX}, can be estimated based on the relationship:

$$G^0_{N,2} = \upsilon_{trapped} \frac{c\,\rho_{melt} RT}{M_{strand}}, \qquad (1)$$

with ρ_{melt} being the density of OEGMA in the melt state and *c*, the concentration of the network, which is equal to 1.6 wt% for all the gels analysed here. The parameter $\upsilon_{trapped}$, which represents the

weight fraction of segments trapped between two active crosslinks, allows accounting for the fact that dangling ends do not participate to the network elasticity. If we consider that all segments contribute to the network (i.e. $\upsilon_{trapped}=1$), a value of 320 kg/mol is found for M_{XX}, which is larger than the average molar mass in number of the chains, M_{chain}, if these ones are not crosslinked. Indeed, if we perform the polymerization with only TMPMP and OEGMA and without $OEGMA_2$ crosslinker, one can estimate M_{chain} as equal to 180 kg/mol, with a molar mass polydispersity of 1.8 as measured by SEC. This large value of M_{XX} suggests that a large fraction of the polymer is not trapped into the network and therefore, does not contribute to the sample elasticity. This is consistent with the observation that at slightly lower crosslinking density, $X_{CL}=0.02$, the sample shows a liquid behavior, the crosslink density being too low to lead to the formation of a network (see Fig. S1).

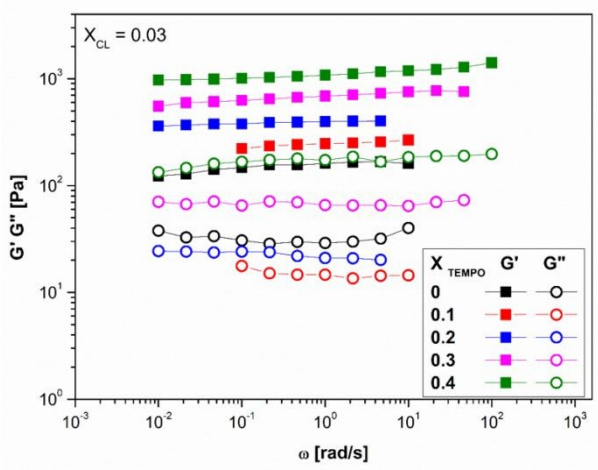

Fig. 6 Frequency sweep plots of storage and loss moduli *versus* frequency for P(TEMPO-*r*-OEGMA) hydrogels with different X_{TEMPO}.

In order to estimate the fraction of dangling ends, a statistical algorithm has been developed,[41] based on the assumptions proposed by Flory: 1) All monomer have the same probability to be a crosslink, 2) this probability does not depend on the position of the other crosslinks along the chain, 3) Intramolecular crosslinks are not taken into account. Starting from the estimated molar mass distribution of the non-crosslinked chains and from the molar mass of a OEGMA unit, equal to 300 g/mol, a large ensemble of chains is generated, along which crosslinkers are included in a statistical way, with a certain probability p_X. The chains composition is then analyzed, which allows us to determine $\upsilon_{trapped}$ and M_{strand} and consequently, the elastic plateau modulus in function of p_X. It must be noted that same results could have been obtained analytically.[42,43] However, due to the sample polydispersity and to the low level of crosslinks per chain, a statistical algorithm has been preferred.[41]

Fig. 7 presents the values of p_X of the different samples, which have been determined such that the corresponding values of $\upsilon_{trapped}$ and M_{strand} lead to the right level of plateau modulus, through Eq. 1 (see insert in Fig. 7).

The corresponding molar mass distributions of free chains, dangling ends and trapped segments are shown in Fig. 8, in case of X_{TEMPO}=0, and compared to the distribution of the non-crosslinked sample (X_{CL}=0). It is found that within this sample, 27.3 wt% of the chains are linear (i.e. with no crosslink), 50 wt% of the chain segments are dangling ends and only $\upsilon_{trapped}$ = 22.7 wt% of the chains segments are trapped between two crosslinks, i.e. only ¼ of the sample contributes to the elastic plateau. This value is in agreement with the fraction of P(OEGMA) chains experimentally extracted from the hydrogel (20.5 wt%). Furthermore, the average molar mass in number of a molecular segment between two crosslinks or chain extremities, M_{strand}, is 87 kg/mol. This molar mass is also in good agreement with the M_n found by SEC analysis of the fraction of non-entrapped chains in the gels (86 kg/mol and $Đ$ of 1.8).

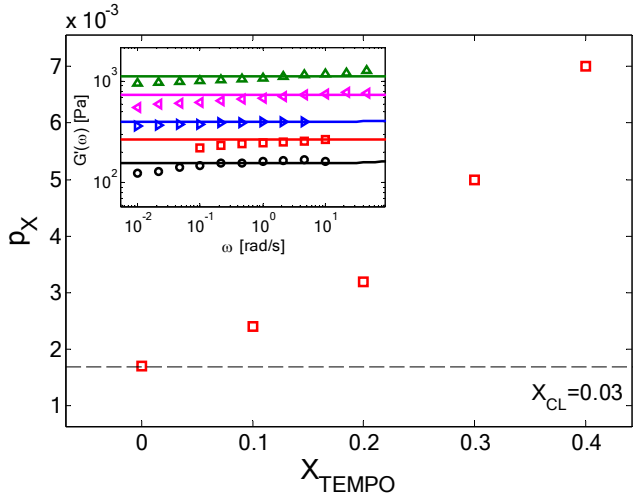

Fig. 7 Crosslinking probability p_X in function of X_{TEMPO}, determined such as the corresponding value of $\upsilon_{trapped}$ and M_{strand} lead to the right level of plateau modulus (see Insert: Experimental (symbols) versus theoretical (line) data, for X_{TEMPO} = 0 (o), 0.1 (□), 0.2 (>), 0.3 (<) and 0.4 (Δ)).

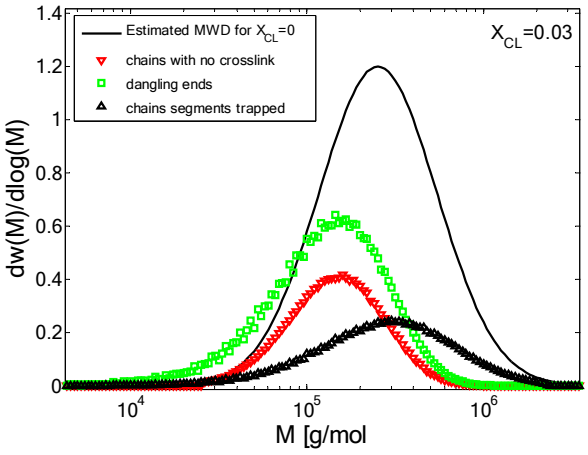

Fig. 8 The sample X_{CL}=0.03 and X_{TEMPO}=0 is divided into several contributions: The MWD distribution of the chains containing zero crosslink, of the dangling ends (excluding the chains with no crosslinks), and of the chain segments trapped between the first and the last crosslinks. For comparison, the MWD of the chains with no crosslink (X_{CL}=0, M_n = 180kg/mol, PDI=1.8) is also presented.

View Article Online
DOI: 10.1039/C9SM00905A

By adding TEMPO units, the storage modulus G' increases (Fig. 6). Since these units are insoluble in water, we hypothesize that TEMPO groups aggregate into hydrophobic domains that could be at the origin of the nanostructures observed by cryo-TEM (Fig. S4, ESI†). As suggested before, those hydrophobic domains could play the role of additional physical crosslinks to the chemical crosslinks provided by $OEGMA_2$ units, which explains the increase in elastic modulus of our hydrogels with increasing X_{TEMPO}.

The constant storage modulus observed for the samples containing TEMPO units means that the lifetime of the corresponding hydrophobic domains is long since their relaxation is not observed within the experimental frequency window. In order to investigate their reversible behaviour, strain sweeps have been performed from low to high strain amplitude and then, from high to low strain. Results are shown in Fig. 9 for X_{TEMPO} = 0.1 and 0.4. For both samples, a hysteresis is observed, which can be seen as a signature of the reversible bonds: while the network structure is partially broken at high strain in order to allow the sample to deform, the network is reformed when coming back to low strain amplitude.

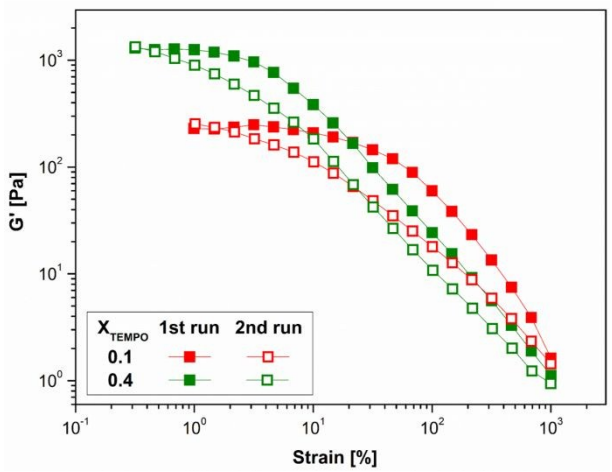

Fig. 9 Storage modulus of the P(TEMPO-*r*-OEGMA) hydrogels with X_{CL}=0.03 and X_{TEMPO}=0.1 (red) or 0.4 (green), from low to high (filled symbols) or high to low (empty symbols) amplitude of deformation.

It is also observed that the hydrogels show a resistance *versus* strain till approximately 10% and 3% with X_{TEMPO}=0.1 and 0.4, respectively, before losing their elasticity (Fig. 9). The lower resistance found with X_{TEMPO}=0.4 is consistent with the fact that the network is denser and therefore, the physical crosslinks have to break at lower strain in order to allow the sample flowing.

Regarding the oxidized form $TEMPO^+$ containing hydrogels, a frequency sweep was performed that confirms gel formation. While comparing the rheological properties of the P(TEMPO-*r*-OEGMA) and P($TEMPO^+$-*r*-OEGMA) hydrogels (Fig. 10), we observe that the charged gel displays higher moduli than the non-charged one. Although the hydrophobic TEMPO domains should disappear upon oxidation of their nitroxide radicals into soluble oxoammonium cations, we hypothesize that the resulting cationic units induce a stretching of the polymer chains due to polyelectrolyte behavior and a stiffening of the gel due to electrostatic repulsions.

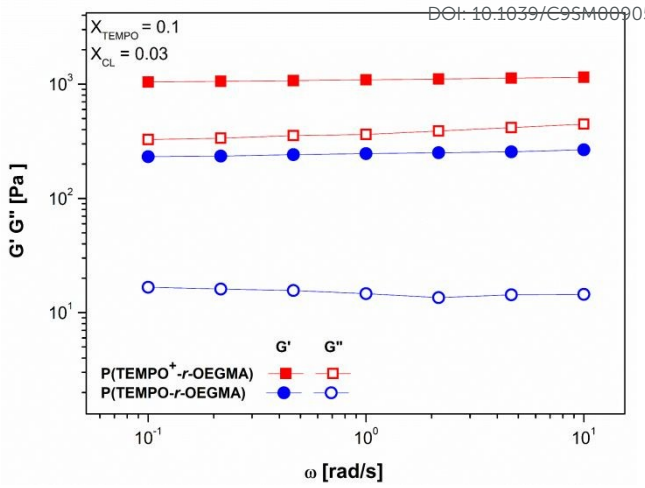

Fig. 10 Frequency sweep plots of storage and loss moduli *versus* frequency for P(TEMPO-*r*-OEGMA) and P($TEMPO^+$-*r*-OEGMA) hydrogels with X_{TEMPO} = 0.1 and X_{CL} = 0.03.

Encapsulation properties

In order to demonstrate the encapsulation abilities of our hydrogels, we have designed a proof-of-concept experiment taking opportunity of the presence of positively charged units in the oxidized P(TEMPO-*r*-OEGMA) hydrogels to encapsulate a negatively charged model molecule, namely eosin B. Eosin B was selected since it is a chromophore that can be easily visually followed by its pink-red color. In a first experiment we used water containing eosin B at a concentration of 5g/L to realize the equilibrium swelling of either the P(TEMPO-*r*-OEGMA) or the P($TEMPO^+$-*r*-OEGMA) hydrogels. As macroscopically observed in Fig. 11, both P(TEMPO-*r*-OEGMA) and the P($TEMPO^+$-*r*-OEGMA) (both prepared from the network with X_{TEMPO} = 0.4 and X_{CL} = 0.03) do form hydrogels with encapsulated eosin B. Nevertheless, the supernatant from the hydrogel prepared from the P($TEMPO^+$-*r*-OEGMA) (Fig. 11a) seems to be colorless while the one from the P(TEMPO-*r*-OEGMA) sample (Fig. 11b) still presents the same characteristic pink color as the one of the starting eosin B solution at t_0. This preliminary observation suggests that some specific interactions are existing between P($TEMPO^+$-*r*-OEGMA) and eosin B that could explain the sequestration of eosin B molecules into the hydrogel. In the case of the P(TEMPO-*r*-OEGMA) hydrogel, eosin B seems to be homogeneously dispersed in the hydrogel and in the supernatant.

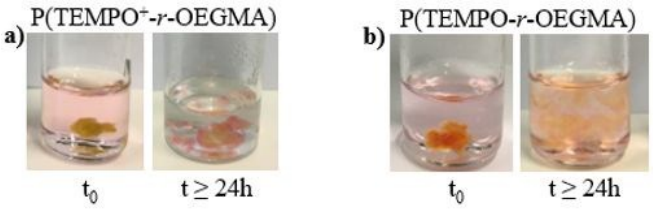

Fig. 11 Encapsulation of eosin B via two strategies a) electrostatic interaction (+/-) b) entrapping in the interior gel network by swelling phenomena (hydrogels prepared from the networks with X_{TEMPO} = 0.4 and X_{CL} = 0.03).

This observation was confirmed by UV-Vis measurements realized on the supernatant after equilibration. As observed in Fig. 12 the characteristic absorption peak of eosin B at 514 nm is still observed in the supernatant of the P(TEMPO-*r*-OEGMA) hydrogel while it totally disappeared in the supernatant of the P(TEMPO$^+$-*r*-OEGMA) sample. This observation points towards strong electrostatic interactions between the charged TEMPO$^+$ units and negatively charged eosin B molecules in the case of the P(TEMPO$^+$-*r*-OEGMA) hydrogel. In the experimental conditions used for this experiment with an initial concentration of $8.619*10^{-3}$ mol/L of eosin B in the aqueous solution used for the swelling process, the concentration of TEMPO$^+$ (0.0013 mol/g) units is sufficient to electrostatically complex the whole eosin B molecules. For the supernatant of the P(TEMPO-*r*-OEGMA) hydrogel the concentration in eosin B drops to $8,421*10^{-7}$ mol/L as determined from Beer-Lambert law. This means an excess of the eosin B molecules are sequestrated into the hydrogels (but not all as in the case of the P(TEMPO$^+$-*r*-OEGMA) hydrogel). Once again, this phenomenon could be explained by the formation of TEMPO hydrophobic domains inside the P(TEMPO-*r*-OEGMA) hydrogel as previously discussed to explain rheological data and cryo-TEM pictures. Some eosin B molecules could be encapsulated into those hydrophobic domains since eosin B also present hydrophobic aromatic groups beside its anionic groups.

In order to release the eosin B molecules entrapped in the P(TEMPO$^+$-*r*-OEGMA) gels, we have tried to screen the electrostatic interactions between TEMPO$^+$ units and negatively charged eosin B. Our attempts were however unsuccessful since addition of high amounts of salts resulted in a decreased solubility of OEGMA units because of salting-out effect.

These preliminary experiments suggest that both P(TEMPO-*r*-OEGMA) and P(TEMPO$^+$-*r*-OEGMA) hydrogels could be useful for further encapsulation/release of molecules of interest.

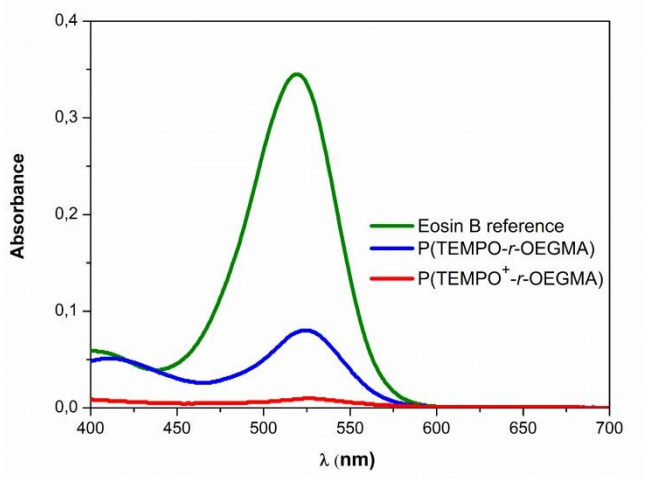

Fig. 12 UV-visible spectra of the supernatant of P(TEMPO-*r*-OEGMA) (blue line) and P(TEMPO$^+$-*r*-OEGMA) (red line) hydrogels after equilibrium swelling in eosin B solution (hydrogels prepared from the networks with X_{TEMPO} = 0.4 and X_{CL} = 0.03).

Conclusions

View Article Online
DOI: 10.1039/C9SM00905A

In this study, the synthesis of redox-responsive hydrogels containing the 2,2,6,6-tetramethyl-1-piperidinyloxy methacrylate (TEMPO methacrylate) monomer has been disclosed. The amine-precursor of this monomer (TMPM) has been combined with oligoethyleneglycol methacrylate (OEGMA) to afford water solubility. The conventional radical polymerization technique used in this study proceeds in the quantitative incorporation of the comonomers into the polymeric network, allowing a perfect control over its composition. The TMPM has been further quantitatively converted into TEMPO methacrylate by a simple oxidation reaction directly performed on the gel. Finally, the TEMPO nitroxide radical can be also quantitatively oxidized to the positively charged TEMPO$^+$ oxoammonium cation. Swelling tests have revealed that the optimum molar fraction of crosslinker, X_{CL}, is equal to 0.03 in order to obtain homogeneous gels displaying high swelling ratios. The amount of TEMPO units (expressed as X_{TEMPO} molar fraction) has been varied in the hydrogels. Cryo-TEM pictures and rheological tests suggest that TEMPO units form hydrophobic domains in the hydrogels. Rheological experiments have confirmed that our hydrogels are slightly chemically crosslinked hydrogels further re-inforced by physically crosslinked nanodomains resulting from the aggregation of hydrophobic TEMPO units.

Finally, the encapsulation abilities of the accordingly formed hydrogels have been explored by using eosin B as a model molecule. It has been demonstrated that the P(TEMPO$^+$-*r*-OEGMA) hydrogel is very efficient to encapsulate eosin B molecules and electrostatic interactions have been anticipated. In the case of the P(TEMPO-*r*-OEGMA) hydrogel, some encapsulation of eosin B has been also monitored. In the latter case, hydrophobic interactions between eosin B and TEMPO domains are hypothesized. Those preliminary results have demonstrated the potential of the investigated hydrogels for further application. Further studies will include a more detailed characterization of the rheological behavior of our hydrogels, the study of the release of guest molecules from either the P(TEMPO-*r*-OEGMA) or P(TEMPO$^+$-*r*-OEGMA) hydrogels and the study of the thermo-responsive behavior of those hydrogels.

Conflicts of interest

There are no conflicts to declare.

Acknowledgements

MK is grateful to the International Relation Offices (ADRI) of UClouvain and to the Concerted Research Action BATTAB (14/19-057) for financing her PhD. JFG is grateful to the Fondation Louvain through the 2018 Marcel de Merre Price for Nanotechnologies for financing this research. SG thanks the Concerted Research Action SlidNet (ARC 16/21-076) for financing his PhD. EVR is researcher qualifié of the F.N.R.S. The authors also thank the Joint Lab for Structural Research at the Integrative Research Institute for the Sciences (IRIS Adlershof).

References

1 E. Caló and V. V. Khutoryanskiy, *Eur. Polym. J.*, 2015, **65**, 252–267.

2 F. Ullah, M. B. H. Othman, F. Javed, Z. Ahmad and H. M. Akil, *Mater. Sci. Eng. C*, 2015, **57**, 414–433.

3 D. Klinger and K. Landfester, *Polymer (Guildf).*, 2012, **53**, 5209–5231.

4 W. Cheng and Y. Liu, *Redox-responsive hydrogels*, Elsevier Ltd, 2017.

5 I. Willner, *Acc. Chem. Res.*, 2017, **50**, 657–658.

6 J. Yun, A. R. Oh, J. S. Im, H. Il Kim and Y. S. Lee, *Macromol. Res.*, 2012, **20**, 1029–1036.

7 P. B. Kajjari, L. S. Manjeshwar and T. M. Aminabhavi, *AAPS PharmSciTech*, 2012, **13**, 1147–1157.

8 S. Namkung and C. C. Chu, *J. Biomater. Sci. Polym. Ed.*, 2007, **18**, 901–924.

9 Y. Li, T. Park, J. K. Quansah and S. C. Zimmerman, *J. Am. Chem. Soc.*, 2011, **133**, 17118–17121.

10 Y. Z. You, Q. H. Zhou, D. S. Manickam, L. Wan, G. Z. Mao and D. Oupický, *Macromolecules*, 2007, **40**, 8617–8624.

11 E. U. Kulawardana, T. Kuruwita-Mudiyanselage and D. C. Neckers, *J. Polym. Sci. Part A Polym. Chem.*, 2009, **47**, 3318–3325.

12 T. Satoh, K. Sumaru, T. Takagi and T. Kanamori, *Soft Matter*, 2011, **7**, 8030–8034.

13 B. S. Kaith, R. Jindal, H. Mittal and K. Kumar, *Der Chem. Sin.*, 2010, **1**, 44–54.

14 D. Schmaljohann, *Adv. Drug Deliv. Rev.*, 2006, **58**, 1655–1670.

15 D. Schmalijohann, J. Oswald, B. Jørgensen, M. Nitschke, D. Beyerlein and C. Werner, *Biomacromolecules*, 2003, **4**, 1733–1739.

16 J. Zhang and N. A. Peppas, *Macromolecules*, 2000, **33**, 102–107.

17 T. Okano, N. Yamada, M. Okuhara, H. Sakai and Y. Sakurai, *Biomater. Silver Jubil. Compend.*, 1995, **16**, 297–303.

18 R. J. Mart, R. D. Osborne, M. M. Stevens and R. V. Ulijn, *Soft Matter*, 2006, **2**, 822–835.

19 R. Hoogenboom, H. M. L. Thijs, M. J. H. C. Jochems, B. M. Van Lankvelt, M. W. M. Fijten and U. S. Schubert, *Chem. Commun.*, 2008, **0**, 5758–5760.

20 S. Glatzel, A. Laschewsky and J. F. Lutz, *Macromolecules*, 2011, **44**, 413–415.

21 J. F. Lutz, *J. Polym. Sci. Part A Polym. Chem.*, 2008, **46**, 3459–3470.

22 S. Sugihara, K. Hashimoto, S. Okabe, M. Shibayama, S. Kanaoka and S. Aoshima, *Macromolecules*, 2004, **37**, 336–343.

23 S. Han, M. Hagiwara and T. Ishizone, *Macromolecules*, 2003, **36**, 8312–8319.

24 M. M. Ali and H. D. H. Stöver, *Macromolecules*, 2004, **37**, 5219–5227.

25 H. Kitano, T. Hirabayashi, M. Gemmei-Ide and M. Kyogoku, *Macromol. Chem. Phys.*, 2004, **205**, 1651–1659.

26 D. Zhang and C. Ortiz, *Macromolecules*, 2004, **37**, 4271–4282.

27 M. Hrubý, S. K. Filippov and P. Štěpánek, *Eur. Polym. J.*, 2015, **65**, 82–97.

28 X. Sui, X. Feng, M. A. Hempenius and G. J. Vancso, *J. Mater. Chem. B*, 2013, **1**, 1658–1672.

29 C. J. Pérez-Martínez, S. D. Morales Chávez, T. Del Castillo-Castro, T. E. Lara Ceniceros, M. M. Castillo-Ortega, D. E. Rodríguez-Félix and J. C. Gálvez Ruiz, *React. Funct. Polym.*, 2016, **100**, 12–17.

30 R. E. Rivero, M. A. Molina, C. R. Rivarola and C. A. Barbero, *Sensors Actuators, B Chem.*, 2014, **190**, 270–278.

31 J. P. Blinco, J. L. Hodgson, B. J. Morrow, J. R. Walker, G. D. Will, M. L. Coote and S. E. Bottle, *J. Org. Chem.*, 2008, **73**, 6763–6771.

32 K. A. Hansen and J. P. Blinco, *Polym. Chem.*, 2018, **9**, 1479–1516.

33 T. Yoshitomi, K. Kuramochi, L. Binh Vong and Y. Nagasaki, *Sci. Technol. Adv. Mater.*, 2014, **15**, 1–7.

34 T. Janoschka, S. Morgenstern, H. Hiller, C. Friebe, K. Wolkersdörfer, B. Häupler, M. D. Hager and U. S. Schubert, *Polym. Chem.*, 2015, **6**, 7801–7811.

35 A. Vlad, N. Singh, J. Rolland, S. Melinte, P. M. Ajayan and J. F. Gohy, *Sci. Rep.*, 2014, **4**, 1–7.

36 J. M. Bobbitt, N. A. Eddy, C. X. Cady, J. Jin, J. A. Gascon, S. Gelpí-Dominguez, J. Zakrzewski and M. D. Morton, *J. Org. Chem.*, 2017, **82**, 9279–9290.

37 O. Bertrand, A. Vlad, R. Hoogenboom and J. Gohy, *Polym. Chem.*, 2016, **7**, 1088–1095.

38 J. M. Bobbitt, *J. Org. Chem.*, 1998, **63**, 9367–9374.

39 Z. Zhai, L. Lei, J. Song, B. Song, X. Pei and Z. Cui, *Soft Matter*, 2016, **12**, 2715–2720.

40 G. Hauffman, J. Rolland, J.-P. Bourgeois, A. Vlad and J.-F. Gohy, *Polym. Chem.*, 2013, **51**, 101–108.

View Article Online
DOI: 10.1039/C9SM00905A

41 L. G. D. Hawke, M. Ahmadi, H. Goldansaz, E. Van Ruymbeke *J. Rheol.,* 2016, **60**, 297-310.

42 D. R. Miller, C. W. Macosko, *J. Polym. Sci. Pol. Phys.,* 1987, **25,** 2441-2469

43 D. R. Miller, C. W. Macosko, *Macromolecules,* 1976, **9**, 206-211.

TOC entry

Redox hydrogels are obtained by introducing into a poly(oligoethyleneglycol)methacrylate network 2,2,6,6-tetramethyl-1-piperidinyloxy radicals that can be oxidized into oxoammonium cations.